Genetic Interactions in Zebrafish Midline Development

Marnie E. Halpern,[1] **Kohei Hatta,**[2] **Sharon L. Amacher, William S. Talbot,**[3]
Yi-Lin Yan, Bernard Thisse,[4] **Christine Thisse,**[5] **John H. Postlethwait,**
and Charles B. Kimmel[6]

Institute of Neuroscience, 1254 University of Oregon, Eugene, Oregon 97403-1254

Mutational analyses have shown that the genes *no tail* (*ntl, Brachyury* homolog), *floating head* (*flh,* a *Not* homeobox gene),
and *cyclops* (*cyc*) play direct and essential roles in the development of midline structures in the zebrafish. In both *ntl* and
flh mutants a notochord does not develop, and in *cyc* mutants the floor plate is nearly entirely missing. We made double
mutants to learn how these genes might interact. Midline development is disrupted to a greater extent in *cyc;flh* double
mutants than in either *cyc* or *flh* single mutants; their effects appear additive. Both the notochord and floor plate are
completely lacking, and other phenotypic disturbances suggest that midline signaling functions are severely reduced. On
the other hand, trunk midline defects in *flh;ntl* double mutants are not additive, but are most often similar to those in *ntl*
single mutants. This finding reveals that loss of *ntl* function can suppress phenotypic defects due to mutation at *flh,* and
we interpret it to mean that the wild-type allele of *ntl* (*ntl*[+]) functions upstream to *flh* in a regulatory hierarchy. Loss of
function of *ntl* also strongly suppresses the floor plate deficiency in *cyc* mutants, for we found trunk floor plate to be
present in *cyc;ntl* double mutants. From these findings we propose that *ntl*[+] plays an early role in cell fate choice at the
dorsal midline, mediated by the Ntl protein acting to antagonize floor plate development as well as to promote notochord
development. © 1997 Academic Press

INTRODUCTION

Genetic control of development of the vertebrate midline
is now beginning to be understood through a combination of
investigative approaches with a variety of organisms (for re-
view see Lemaire and Kodjabachian, 1996). The most promi-
nent of the midline tissues, the notochord, signals develop-
ment of the floor plate, a tissue that immediately overlies the
notochord, in the ventral midline of the central nervous sys-
tem (CNS) (reviewed in Jessell and Dodd, 1992; Placzek, 1995).
Together the notochord and floor plate serve as a polarizing
center, organizing development of nearby cell types including
motor neurons and somitic derivatives (Yamada *et al.,* 1991,
1993; Placzek *et al.,* 1993; Beattie *et al.,* 1997; reviewed by
Placzek, 1995; Cossu *et al.,* 1996). Many studies have impli-
cated Hedgehog proteins as important signaling molecules in
these induction events (reviewed by Placzek *et al.,* 1995; Ham-
merschmidt *et al.,* 1997).

Both the notochord and the floor plate originate from
the same precursor dorsal ''organizer'' region in the early
embryo, which in zebrafish can be readily recognized just
after gastrulation begins by a distinctive accumulation of
cells, the embryonic shield (Kimmel *et al.,* 1995). Cell lin-
eage analyses suggest that by this stage cells of the organizer
region have already been specified to develop particular tis-
sue types (Shih and Fraser, 1995; Melby *et al.,* 1996), and are
under control of zygotically expressed genes (for example,
goosecoid, Stachel *et al.,* 1993; Thisse *et al.,* 1994; *no tail*
(*Brachyury* homolog), Schulte-Merker *et al.,* 1992; *axial*
(*HNF3β* homolog), Strahle *et al.,* 1993; *myoD,* Weinberg *et*

al., 1996; *twist,* Halpern *et al.,* 1995; *floating head* (a *Not* homeobox gene), Talbot *et al.,* 1995; Melby *et al.,* 1996).

Mutational analyses in zebrafish have identified a number of genes, including *cyclops* (*cyc*), *no tail* (*ntl*), and *floating head* (*flh*), as playing essential roles in midline development (Hatta *et al.,* 1991; Halpern *et al.,* 1993, 1995; Talbot *et al.,* 1995). Loss of function of *cyc* nearly entirely deletes the floor plate, in addition to other defects including deficiencies in the prechordal plate, the notochord, and ventral–anterior regions of the CNS (Hatta *et al.,* 1991, 1994; Hatta, 1992; Krauss *et al.,* 1993; Strahle *et al.,* 1993; Ekker *et al.,* 1995; Ungar *et al.,* 1995; Yan *et al.,* 1995; Allende and Weinberg, 1994; Thisse *et al.,* 1994; Barth and Wilson, 1995; Macdonald *et al.,* 1995; Toyama *et al.,* 1995; Hauptmann and Gerster, 1996; Warga, 1996). The molecular identity of *cyc* is unknown. *ntl* is orthologous to *Brachyury,* a gene well known from studies in mouse and *Xenopus,* and with homologs known in a variety of other species (Halpern *et al.,* 1993; Schulte-Merker *et al.,* 1994; Herrmann and Kispert, 1994; Kispert *et al.,* 1994; 1995b; Yasuo and Satoh, 1993; 1994; Harada *et al.,* 1995; Holland *et al.,* 1995). The *Brachyury/ntl* gene encodes a putative transcription factor that is expressed in the rudiments of both notochord and tail, and is essential for development in both domains (Kispert and Herrmann, 1993; 1994; Kispert *et al.,* 1995a,b; Conlon *et al.,* 1996; Wilkinson *et al.,* 1990; Smith *et al.,* 1991; Schulte-Merker *et al.,* 1992; Chesley, 1935; Halpern *et al.,* 1993). Loss of *Brachyury/ntl* function appears to disrupt morphogenesis of mesoderm during gastrulation in both mouse and zebrafish (Wilson *et al.,* 1995; Melby *et al.,* 1997). Notochord differentiation is blocked, completely in zebrafish and perhaps incompletely in the mouse (Chesley *et al.,* 1935; Herrmann, 1991; Halpern *et al.,* 1993; Wilson *et al.,* 1995; Rashbass *et al.,* 1994). *flh* is a *Not* homeobox gene with homologs known in *Xenopus* and chicken (von Dassow *et al.,* 1993; Gont *et al.,* 1993; Knezevic *et al.,* 1995; Stein and Kessel, 1995; Stein *et al.,* 1996). In the early zebrafish gastrula *flh* is expressed in precursors of the notochord, and in this domain it functions to promote notochord development and to repress muscle development (Talbot *et al.,* 1995; Halpern *et al.,* 1995; Melby *et al.,* 1996). Gain-of-function experiments in *Xenopus* show that overexpression of *Xnot-2* leads to an expanded notochord at the expense of nearby mesoderm, particularly somitic mesoderm (Gont *et al.,* 1996). In *flh* mutants during gastrulation, cells occupying the notochord domain lose the normal features of notochord precursors and they differentiate as muscle (Halpern *et al.,* 1995; Melby *et al.,* 1996).

The objective of our work is to learn how genes control cell fate decisions in the newly emerging vertebrate embryonic axis. At midbody levels *cyc, ntl,* and *flh* mutants each have distinctive phenotypes that appear to be due to different defects in the development of cells deriving from the same area, the organizer region, of the early gastrula. Here we describe the use of double mutants to investigate possible interactions between these genes. We find that loss of function of *cyc* and *flh* combine additively to very severely disrupt the embryonic midline, including its signaling functions. On the other hand, at the same midbody levels *ntl* is epistatic to both *cyc* and *flh,* revealing prominent genetic interactions. The findings motivate a new hypothesis that the wild-type *ntl* gene functions in the cell fate choice between notochord and floor plate.

MATERIALS AND METHODS

Fish and Mutant Lines

Fish were reared at 28.5°C and cared for as previously described (Westerfield, 1994). Embryos were obtained from matings between pairs of fish singly or doubly heterozygous for the mutant alleles being examined. Embryos were collected, sorted into embryo medium (EM; Westerfield, 1994), and maintained at 28.5°C until the appropriate developmental stage. Staging criteria of Kimmel *et al.* (1995) were followed.

The *cyc* (cyc^{b16}, cyc^{b213}, and cyc^{b229}) and ntl^{b160} mutant alleles used in this study were γ-ray induced. The ntl^{b195} mutation arose spontaneously and results from a DNA insertion in the Ntl protein coding sequence (Schulte-Merker *et al.,* 1994). flh^{n1} is also a spontaneous mutation, resulting from a 2-base-pair deletion in the coding sequence upstream of its homeobox (Talbot *et al.,* 1995). The genes are unlinked to one another; *cyc* maps to linkage group 12, *flh* to linkage group 13, and *ntl* to linkage group 19 (Postlethwait *et al.,* 1994). To produce parental fish that were heterozygous at two of the loci, fish heterozygous for one of the mutations were mated to fish heterozygous for the other, and the progeny were reared. The double heterozygotes were identified by single pair matings, and subsequently intercrossed to obtain homozygous double mutant embryos.

cyc;flh double mutants were produced using the cyc^{b16} and flh^{n1} alleles. The intercross progeny of double heterozygotes fell into four phenotypic classes (WT:cyc^-:flh^-:cyc^-;flh^-) exhibiting ratios not significantly different from the 9:3:3:1 ratio expected for independently sorting (Mendelian) genes (9.67:2.76:2.49:1.09, $n = 662$, $\chi^2 = 6.08$, $P > 0.1$).

We obtained *flh;ntl* double mutants using the flh^{n1} allele with either ntl^- allele, mostly ntl^{b195}. From intercrosses of doubly heterozygous fish, we could easily sort three phenotypic classes (WT, flh^-, ntl^-) in a ratio of 9:3:4 as expected from independent assortment and assuming that *ntl* is epistatic to *flh* (8.89:3.14:3.97, $n = 612$, $\chi^2 = 0.297$, $P > 0.7$). Upon closer inspection of ntl^- embryos, we observed some individuals that had short stretches of medially fused somites, a flh^--like characteristic; we presumed that these individuals were double mutants. However, the four phenotypic classes (WT:flh^-:ntl^-:flh^-;ntl^-) exhibited a ratio that was significantly different from the expected 9:3:3:1 (8.89:3.14:3.58:0.39, $n = 612$, $\chi^2 = 18.73$, $P < 0.001$). We used allele-specific primers in PCR reactions to confirm that individuals from the double mutant phenotypic class were homozygous for the flh^{n1} allele and to search for individuals within the ntl^- phenotypic class that were homozygous for the flh^{n1} allele. Using this analysis, we found that the ratio of ntl^-:flh^-;ntl^- was 3:1 as expected (3.06:0.94, $n = 149$, $\chi^2 = 0.19$, $P > 0.5$). For PCR analysis, genomic DNA was prepared either from whole zebrafish embryos or from heads of embryos that had undergone *in situ* hybridization. DNA was prepared as described

(Johnson *et al.,* 1994), except 1× Thermopol buffer (New England Biolabs) plus 1 mg/ml proteinase K (Boehringer-Mannheim) was used as the digestion buffer and *in situ* hybrized embryos were washed twice in 1× Thermopol buffer before proteinase K addition. Two separate amplification reactions using allele-specific primers for either the *flh^{n1}* allele or the wild-type *flh* allele were used to determine the genotype of each *ntl^-* embryo. These primers take advantage of a 2-bp deletion in the *flh^{n1}* allele (Talbot *et al.,* 1995). The forward allele-specific primer sequences are 5′-TCTCCAGCT-CTGCGCTCG-3′ (*flh^{n1}* coding strand) and 5′-TCTCCAGCTCTG-CGCTCC-3′ (wild-type *flh* coding strand) and the common reverse primer sequence is 5′-AACTGCTGCTTTCGCCAG-3′ (noncoding strand); both primer pairs amplify a 284-bp product. In addition, an internal common forward primer with sequence complementary to both alleles (5′-CGTGGAGCTGTGTACGCA-3′) was used in each reaction as a control for DNA quality; this primer in combination with the reverse primer produces a 156-bp product. Typically, about 0.4% (whole embryos) or 10% (*in situ* hybridized embryos) of the total genomic DNA sample was used in each PCR reaction. Reaction components and concentrations are as described (Johnson *et al.,* 1994; Postlethwait *et al.,* 1994). PCR conditions were 94°C for 2 min, followed by 40–44 cycles of 94°C for 30 sec, 58°C for 30 sec, 72°C for 30 sec, followed by 72°C for 7 min. Amplified products were separated by electrophoresis on agarose gels.

cyc;ntl double mutant progeny from the intercrosses fell into four distinct phenotypic classes: WT, *cyc^-*, *ntl^-*, and *cyc^-;ntl^-*, which for crosses involving *cyc^{b16}* and *ntl^{b160}* or *cyc^{b229}* and *ntl^{b195}*, exhibited Mendelian ratios of 9:3:3:1. (For *cyc^{b16}/+;ntl^{b160}/+* intercrosses, the ratios were 9.0:2.84:3.11:1.05, $n = 2,873$, $\chi^2 = 2.6$, $P > 0.5$, and for *cyc^{b229}/+;ntl^{b195}/+* intercrosses the ratios were 8.83:3.26:2.88:1.03, $n = 467$, $\chi^2 = 0.89$, $P > 0.7$). In the case of *cyc^{b213}*, which is due to a reciprocal translocation that produces an earlier noncyclopic lethal phenotype referred to as ''severe'' in addition to phenotypically *cyc^-* embryos (W. Talbot, unpublished data), segregation ratios were aberrant and fewer double mutants were observed (WT = 601, severe = 20, *cyc^-* = 11, *ntl^-* = 209, *cyc^-;ntl^-* = 7).

Whole-Mount in Situ Hybridization

Embryos were processed for whole-mount *in situ* hybridization as described (Oxtoby and Jowett, 1993, Thisse *et al.,* 1993). Digoxygenin RNA antisense probes were synthesized by T7 polymerase (Boehringer Mannheim) from a *Hin*dIII-linearized *sonic hedgehog* template (Krauss *et al.,* 1993) or an *Xba*I-linearized *myoD* template (Weinberg *et al.,* 1996), and by T3 polymerase (Boehringer Mannheim) from an *Xho*I-linearized *α-collagen type II* template (*col2a1,* Yan *et al.,* 1995). Embryos were sorted and dechorionated prior to fixation and approximately 10–20 embryos of a given phenotypic class were used for each hybridization. Each experiment was repeated at least twice with the exception of the *cyc^{b213};ntl^{b160}* double mutants which were difficult to obtain due to the aberrant segregation of the *cyc^{b213}* translocation. Following probe visualization, individual embryos were dehydrated in methanol:PBS (50:50) followed by 100% methanol, briefly treated with methyl salicylate or benzyl alcohol:benzyl benzoate (1:2), mounted between coverslips in Permount (Fisher), and photographed on a Zeiss Universal microscope.

For preparation of semithin sections, following probe visualization, embryos were dehydrated through a methanol series to propylene oxide:Epon (1:1) and pure Epon, as described (refer to Westerfield, 1994). Serial sections (7 mm) were dried onto glass slides

and coverslipped under Permount (Fisher). Sections were examined on a Zeiss Axioskop under a 40× water immersion lens and photographed using a color digitizing camera (Kontron). Images were processed using Adobe Photoshop on a Macintosh Quadra 950 with a Nuvista video board.

Immunohistochemistry

Antibody labeling of embryos was performed as described (Halpern *et al.,* 1993). Mouse monoclonal antibody zn-1 (Trevarrow *et al.,* 1990) was used to label ic interneurons. Zn-12 (Trevarrow *et al.,* 1990), recognizing the antigen HNK-1 (Metcalfe *et al.,* 1990) was used to visualize the medial longitudinal fascicles and other CNS structures. Zn-5, recognizing the DMgrasp protein (Kanki *et al.,* 1994; Fashena, 1996) was used to label the floor plate.

Mapping of cyc^{b213}

The mapping of *cyclops,* the linkage group 12 centromere, and most of the other loci shown in Fig. 2 have been described (Postlethwait *et al.,* 1994; Johnson *et al.,* 1996; Knapik *et al.,* 1996; Postlethwait *et al.,* in preparation). The locations of markers z1804 and 15T.750 were determined in various haploid mapping crosses as described (Postlethwait *et al.,* 1994). Primers for the z1804 locus were obtained from Research Genetics. The 15T.750 marker was initially identified as a RAPD marker linked to *cyclops* and was subsequently converted to a sequence-tagged site (STS) by contructing primers corresponding to the sequence of the cloned RAPD fragment. The 15T.750 STS primers are 5′-ACAAACAGAAAT-GGGAATACATAG-3′ and 5′-TTCACAGTATGTGGGATAATA-TTTT-3′. To characterize the *cyc^{b213}* allele, genomic DNA prepared from individual haploid progeny of a female heterozygous for *cyc^{b213}* was pooled and analyzed by PCR using linkage group 12 markers as described (Postlethwait *et al.,* 1994).

RESULTS

The cyc, flh, and ntl Alleles Are Probably Null Mutations

The overall appearances of the mutants are shown in Fig. 1. The single mutant phenotypes have all been described previously (see Introduction for references). With the exception of *cyc^{b213}* (see below), all of the mutations show Mendelian segregation, and intercrosses between double heterozygotes yielded homozygous double mutants in the expected ratios (see Materials and Methods). To interpret meaningfully epistatic interactions between the genes we want to make double mutants that combine severe, loss-of-function alleles (Avery and Wasserman, 1993). The deduced protein sequences encoded by the mutant alleles *ntl^{b160}*, *ntl^{b195}*, and *flh^{n1}* suggest that the gene products are likely to lack function (Schulte-Merker *et al.,* 1994; Talbot *et al.,* 1995). The phenotype of an embryo in which *flh^{n1}* is placed *in trans* to a deficiency also suggests *flh^{n1}* is a null allele (Talbot *et al.,* 1995). The *cyc* gene has not been identified; hence, we have no direct molecular evidence for the nature of the *cyc* alleles
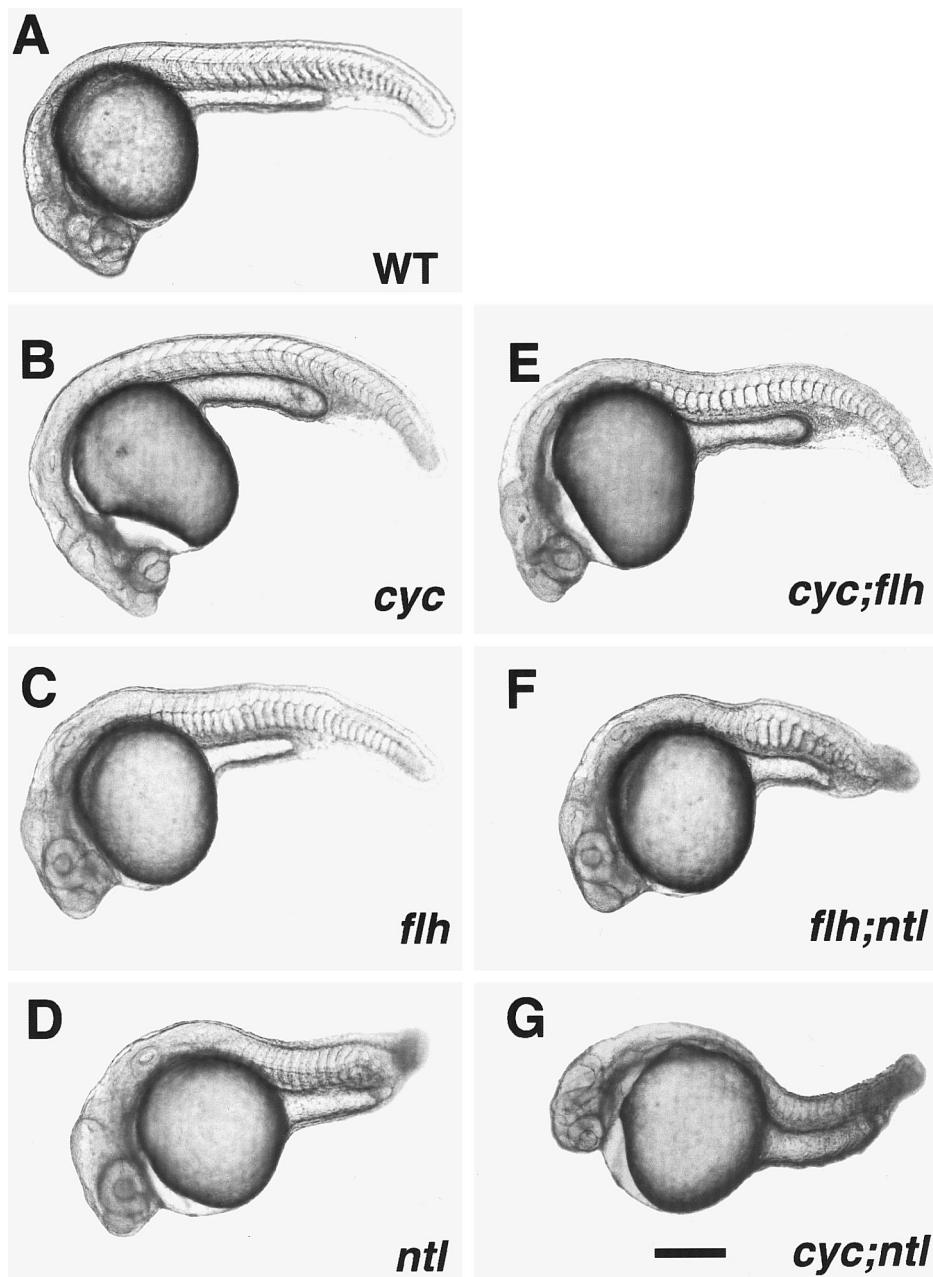
FIG. 1. Pharyngula (24 hr) wild-type (WT, A) and mutant embryos (B–G, the gene name abbreviations on this and other figures indicate homozygous mutants for the loci indicated). The head of the *cyc;flh* double mutant (E) is similar to *cyc⁻* (B; see Hatta *et al.,* 1991), whereas the body is similar to *flh⁻* (C), with respect to both midline somite fusion and lack of ventral body curvature. The tail of the *flh;ntl* double mutant (F) is like *ntl⁻* (D), and in this example there is a patch of fused somites, as present in *flh⁻*, just dorsal to the yolk extension. Somite fusion is variable, occurring in 43% (15/35) of embryos subsequently confirmed to be *flh;ntl* double mutants by PCR genotyping (see Materials and Methods). The *cyc;ntl* double mutant (G) combines the *cyc⁻* head and *ntl⁻* tail phenotypes. Scale bar, 250 μm.

we have studied. We now provide genetic evidence that they are also null mutations.

This interpretation derives from mapping analysis of one of the *cyc* alleles, *cyc^{b213}*, that shows it to be a deficiency of the *cyc* locus (Fig. 2). The *cyc* gene maps to the distal end of linkage group 12 (Postlethwait *et al.,* 1994).
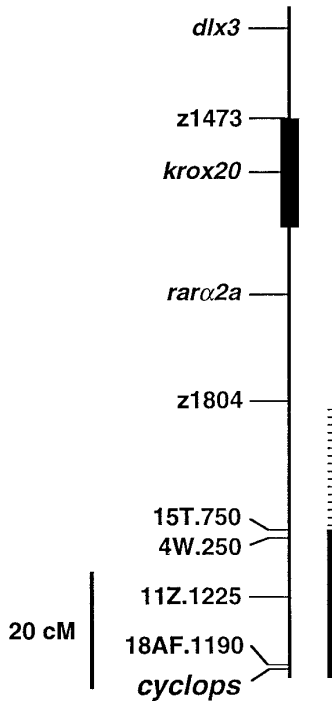
FIG. 2. Genetic mapping establishes that cyc^{b213} is a null mutation. The map positions of the centromere (box containing *krox20*), *cyclops,* and other loci on this linkage group are shown. The black bar indicates the distal region that contains markers that are not present in genomic DNA from cyc^{b213} mutants. The cyc^{b213} translocation breakpoint is located in the region between markers z1804 and 15T.750 (stippled bar).

Molecular markers identifying this region are missing from genomic DNA prepared from cyclopic haploid embryos bearing the cyc^{b213} allele (data not shown). The deleted region in the mutant DNA includes the sequence tagged site denoted 15T.750 and the 3 markers shown distal to 15T.750 in Fig. 2. Markers for the proximal region of linkage group 12 are not deleted in cyc^{b213} (e.g., z1804 in Fig. 2). Additional mapping data indicate that the distal region, containing the *cyc* gene, is translocated to linkage group 2 (Talbot *et al.,* in preparation), the breakpoint residing 25–35 cM proximal to *cyc.*

Diploid homozygotes for the cyc^{b213} deficiency have the severe phenotypic changes resembling homozygotes for cyc^{b16} and cyc^{b229}, that we also utilized in this study. We have not detected phenotypic differences among these mutant alleles. Based on these analyses we conclude that all of the *cyc* mutant alleles, as well as those of *ntl* and *flh,* produce null, or near null phenotypes.

The Combined Effects of cyc⁻ and flh⁻ Severely Disrupt Midline Development

Mutation of either *cyc* or *flh* disrupts both notochord and floor plate development, but the phenotypes of the single
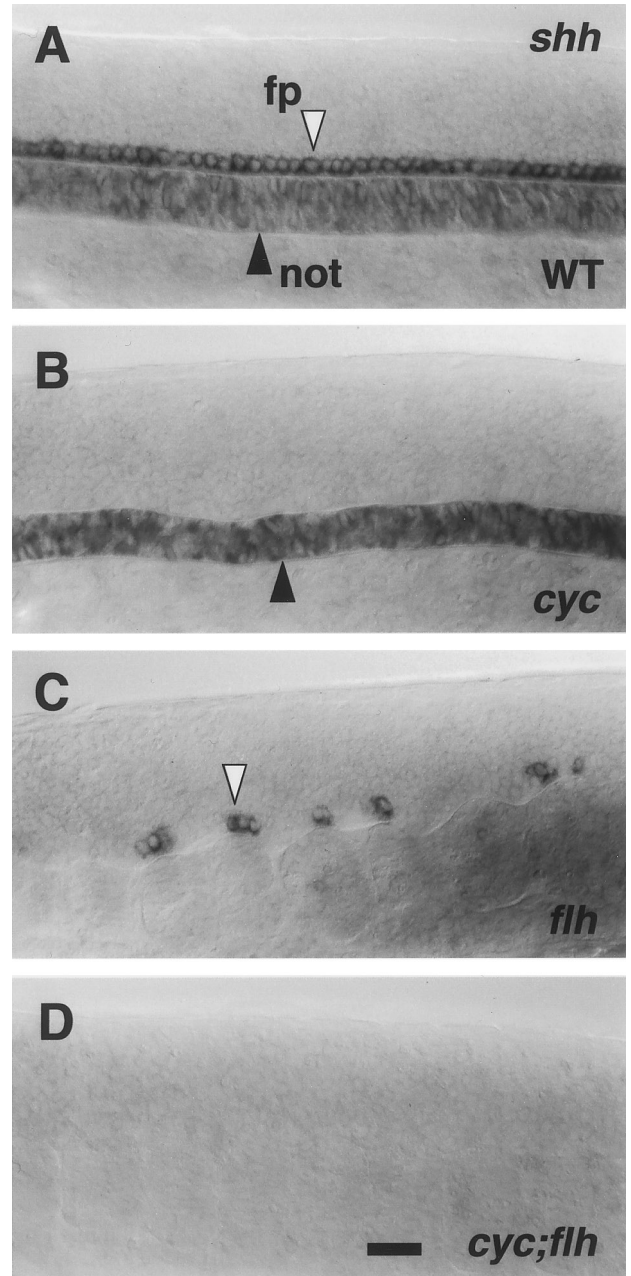

FIG. 3. Expression of *shh* is missing in the trunk midline in *cyc;flh* double mutants at the late segmentation period. Whole-mounted embryos at 21 hr, left side views, with anterior to the left and dorsal to the top. RNA *in situ* hybridization. At this stage in wild-type embryos (A) the floor plate (fp, white arrowhead) expresses *shh* strongly, and expression is becoming downregulated in the notochord (not, dark arrowhead), as previously shown by Krauss *et al.* (1993). The embryos are overstained to reveal weaker levels of notochord *shh* expression. In *cyc* mutants (B) only the notochord is labeled (Krauss *et al.,* 1993), in *flh* mutants (C) only isolated clusters of floor plate cells are labeled (Talbot *et al.,* 1995), and in *cyc;flh* double mutants (D), there is no labeling at all. Scale bar, 25 μm.

mutants (i.e., *cyc⁻* and *flh⁻*) are distinct (Fig. 3). By morphology as well as by expression of several molecular markers scored at 24 hr, the floor plate is nearly completely missing in *cyc⁻*, with a few floor plate cells remaining in the tail of some but not all individuals (Hatta, 1992; Krauss *et al.,* 1993; Yan *et al.,* 1995). Notochord develops in *cyc⁻*, but it is thinner than normal (Warga, 1996; E. Melancon, unpublished results). In contrast to *cyc⁻*, more floor plate is present along the axis in *flh* mutants, but it is disrupted into patches in the spinal cord (Halpern *et al.,* 1995; Talbot *et al.,* 1995) that we term floor plate ''islands'' (see also Beattie *et al.,* 1997). Notochord is entirely lacking in *flh* mutants (Talbot *et al.,* 1995).

The *cyc;flh* double mutants (i.e., embryos homozygous for both mutant alleles) are easily recognized because they bear key phenotypic features of both single mutants, particularly the cyclopia characteristic of *cyc⁻*, and the complete lack of notochord accompanied by somite fusion across the midline characteristic of *flh⁻* (Fig. 1). Floor plate markers failed to label any cells in the ventral neural tube of *cyc;flh* double mutants (Fig. 3). Hence, both differentiated notochord and floor plate seem to be completely missing in *cyc;flh* double mutants. The midline phenotype appears additive.

We observe other defects involving the hindbrain and spinal cord in the *cyc;flh* double mutants that are substantially nonadditive; rather they are dramatically more severe than in either single mutant. A typical example is the change in patterning of a class of ventrally located interneurons termed ic cells that are present in the caudal hindbrain (Fig. 4). In wild-type embryos these cells are present in a bilateral pair of rows, positioned adjacent to the medial longitudinal fascicles, the axonal pathways to which they contribute their axons (Mendelson, 1986). They also form a bilateral pair of rows in *cyc* and *flh* single mutants, located slightly closer to the midline in each single mutant than in the wild type. However, in the *cyc;flh* double mutant ic neurons are present in a single (unpaired) cell row, located just at the midline.

Other examples of nonadditive severe defects in *cyc;flh* mutants include disruption of the axonal pathway of the Mauthner neuron (a giant interneuron in the fourth rhombomere), and disorganization of the lateral longitudinal fascicle that projects rostrocaudally through the length of the hindbrain (data not shown). There are also deficiencies of spinal motoneurons, reported in the accompanying paper (Beattie *et al.,* 1997). It is likely that all of these changes in the nervous system are secondary, nonautonomous effects of the mutations resulting from midline signaling deficiencies (see Discussion).

Variable Epistasis between *flh* and *ntl*

Both *flh* and *ntl* single mutants lack a differentiated notochord. In *flh⁻*, somites are fused medially all along the length of the trunk. In *ntl⁻*, the tail is absent and somite
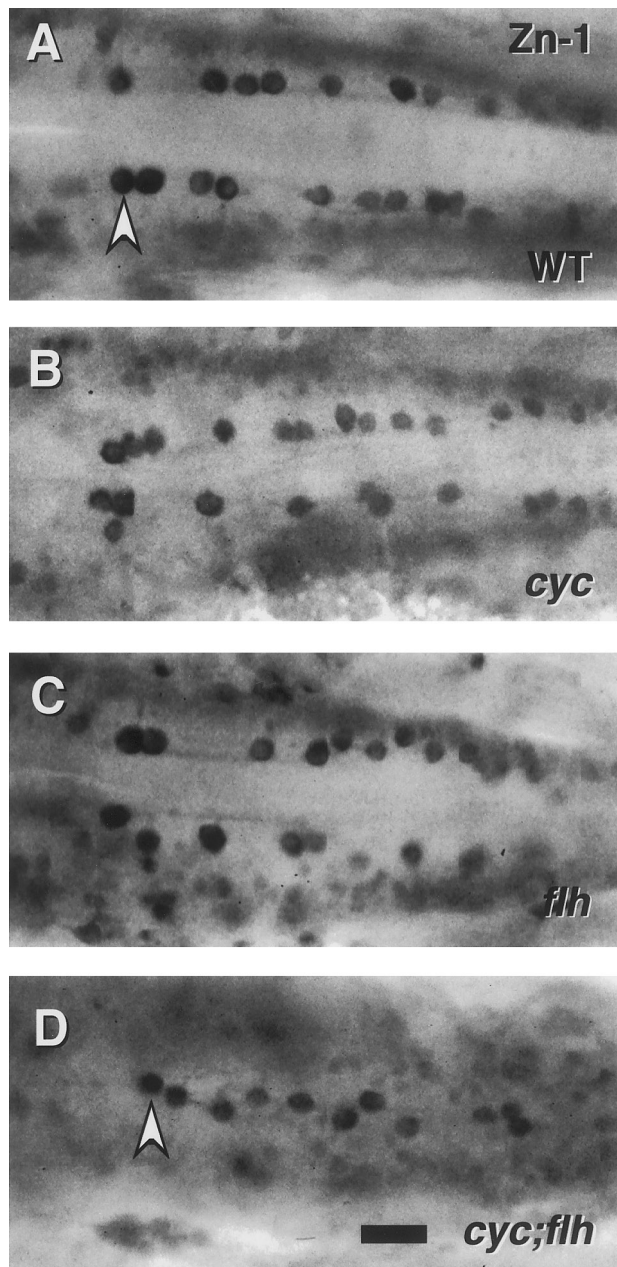

FIG. 4. Patterning of ic interneurons is severely disrupted in *cyc;flh* double mutants. Dorsal views of the caudal hindbrain, with anterior to the left, in whole-mounted embryos labeled with the zn-1 monoclonal antibody at 24 hr. This antibody binds a neuronal antigen that is prominently expressed by ic interneurons, a distinctive class of neurons cells present in the caudal hindbrain that project axons ipsilaterally and caudally, within the medial longitudinal fascicles, to the spinal cord (Mendelson, 1986). In the wild type (A) the ic neurons (arrowhead) line up in bilateral rows adjacent to the medial longitudinal fascicles. The same two cell rows are present (and are closer together) in *cyc* (B) and *flh* (C) single mutants. Only a single disorganized row of ic cells is present, just at the midline, in the *cyc;flh* double mutant (D). Scale bar, 25 µm.

fusion occurs only in a few (3–5) of the caudalmost remaining body segments. Considering the single mutant phenotypes and the expression domains of the two genes, we expected that *flh;ntl* double mutants should sort along with *ntl* single mutants scored by missing tail (Fig. 1). We verified this prediction by using allele-specific PCR primers to identify *flh* homozygous mutants at the expected frequency within this *ntl⁻* phenotypic class (see Materials and Methods). Moreover, we could find live mutant embryos that had patches of fused somites in the trunk (Fig. 1); upon PCR genotyping, these embryos were always double mutants. However, in other cases we could not detect such patches of somite fusion; i.e., the *flh;ntl* double mutant phenotype and the *ntl* single mutant phenotype were indistinguishable. Hence, the midline phenotype is variable among individual *flh;ntl* double mutants. We encountered variability irrespective of whether the double mutants were made with the ntl^{b160} or the ntl^{b195} alleles.

Examination of *myoD* expression provides a sensitive way to analyze further the extent of somitic fusion in the midline of *flh;ntl* double mutants (Fig. 5). The *myoD* gene is first expressed during gastrulation of wild-type embryos, in bilateral patches that flank the axis. Gastrula expression is missing in *ntl* mutants, but then appears in bilateral stripes after gastrulation, similar to the wild-type pattern, although the stripes are more separated (Weinberg *et al.,* 1996; Odenthal *et al.,* 1996). In contrast, *myoD* is expressed in early *flh* mutants, approximately at the correct locations. Then, before the end of gastrulation in *flh* mutants, expression appears ectopically in the midline, fusing the two bilateral stripes together (Halpern *et al.,* 1995). We observed that in *flh;ntl* double mutants examined during the late segmentation period, prominently separated, bilateral *myoD* stripes predominated along the axis, as in *ntl* mutants (Fig. 5). This result, a *myoD* phenotype resembling *ntl⁻*, was already striking at the beginning of the segmentation period (1–2 somite stages, data not shown). However, along the trunk of some individual *flh;ntl* double mutants fixed at the later stage (20 somites) there was a region of midline fusion of the *myoD* stripes, such as is characteristic of the entire length of the trunk in *flh* mutants. These findings show that with respect to *myoD* expression, *ntl* is epistatic to *flh* in most embryos, but that in some individuals (see legend to Fig. 5 for quantification), epistasis reverses in regions that are sometimes several somites long.

The phenotype of the floor plate provides another test of epistasis between *flh* and *ntl* (Fig. 6). As described above, only isolated islands of floor plate persist within the spinal cord of *flh* mutants (Talbot *et al.,* 1995; Odenthal *et al.,* 1996). The floor plate is present and continuous along most of the length of the axis of *ntl* mutants (Halpern *et al.,* 1993), and as revealed by expression of markers such as *shh,* or a collagen gene *col2a1* (Figs. 6F and 7; Krauss *et al.,* 1993; Yan *et al.,* 1995), we found that the floor plate is widened, containing substantially more cells along a given length of the trunk spinal cord in *ntl* mu-
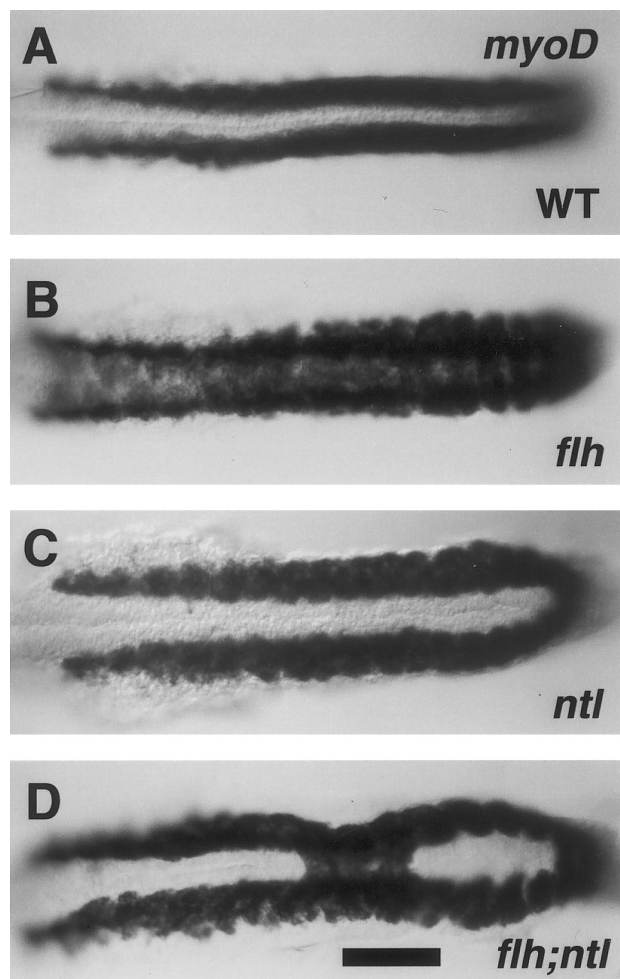

FIG. 5. *ntl⁻* partially suppresses somitic fusion due to *flh⁻*. Dorsal views, with anterior to the left of 19-hr embryos (20-somite stage). RNA *in situ* hybridization for *myoD* (Weinberg *et al.,* 1996). In wild-type embryos (A), bilateral stripes of labeling are present in the trunk beside the developing notochord, which is unlabeled at the midline. In *flh* mutants (B) labeling spreads across the midline, whereas in *ntl* mutants (C) the stripes are distinctively farther apart than in the wild type (Odenthal *et al.,* 1996). Labeling in the *flh;ntl* double mutant is generally *ntl⁻*-like, but a single patch of tissue, involving three adjacent segments, shows the *flh⁻*-like pattern. Forty-six percent of the double mutants ($n = 13$) had fusion of *myoD* expression that included regions of 2–5 somites (mean, 3.2 somites; $n = 6$) at midtrunk levels. The other *flh;ntl* double mutants were indistinguishable from *ntl⁻*. Genotyping of *flh* alleles was performed on all *ntl* mutant and *flh;ntl* mutant embryos by PCR analysis. Scale bar, 100 μm.

tants than in wild-type embryos (Odenthal *et al.,* 1996). In *flh;ntl* double mutants (Figs. 6G and 6H) the floor plate is present through most of the trunk spinal cord. It is nearly continuous along this length, as in *ntl⁻*, and nearly
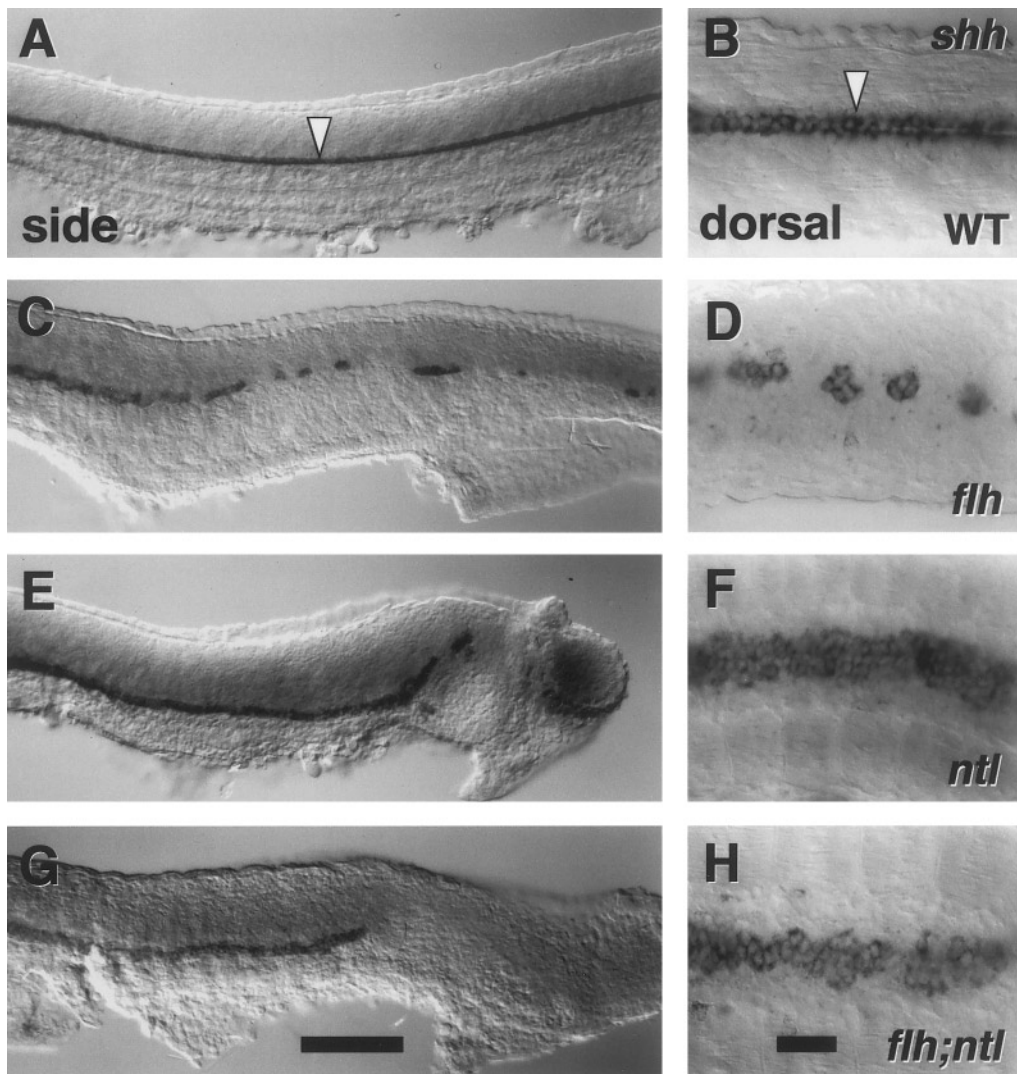
FIG. 6. *ntl⁻* partially suppresses the *flh⁻* floor plate defect. Side views, with anterior to the left. The left panels show matched left side views, with dorsal to the top. The right panels show dorsal views at higher magnification. RNA *in situ* hybridization for *shh* (Krauss *et al.,* 1993). In wild-type embryos (A, B), a one-cell-wide row of floor plate is labeled along the length of the trunk and tail (arrowheads). The floor plate is disrupted into islands of cells in *flh* mutants (C, D; 8 of 50 *flh* mutants had more significant stretches of continuous floor plate labeling than in the example shown). In *ntl* mutant floor plate is present along most of the length of the trunk, except for the caudalmost region (last 1–3 somites, E; we also observed caudal plate to be forked in about half the *ntl* mutants, and interrupted caudally in 8 of 50). The *ntl* mutant floor plate is 3–4 cells wide (F). Floor plate is present along most of the trunk in *flh;ntl* double mutants. Compared with *ntl* mutants, the caudal disruption of the floor plate is more extensive in the *flh;ntl* double mutant (floor plate is lacking in the caudalmost 4–8 somites (G). We also observe local regions along the trunk where the floor plate is disrupted in individual double mutants (not shown). Otherwise, *shh* labeling in *flh;ntl* double mutants is generally *ntl⁻*-like, including substantial floor plate widening (H). We observed the same floor plate phenotypes in these mutants with the marker *col2a1* (data not shown). Scale bars, 100 µm (left panels), 25 µm (right panels).

as wide as the floor plate in *ntl⁻*. Hence, loss of *ntl* function strongly suppresses the *flh⁻* floor plate deficiency. However, one or a few discontinuities are occasionally observed in the *flh;ntl* double mutant floor plate, and floor plate markers are consistantly absent in a longer region of the caudalmost spinal cord of the *flh;ntl* double mutants as compared with *ntl* mutants (5–8 somites vs 1–3 somites). The expressivity of the latter phenotype is sufficient to permit us to unambiguously distinguish between *flh;ntl* double mutants and *ntl* single mutants (as
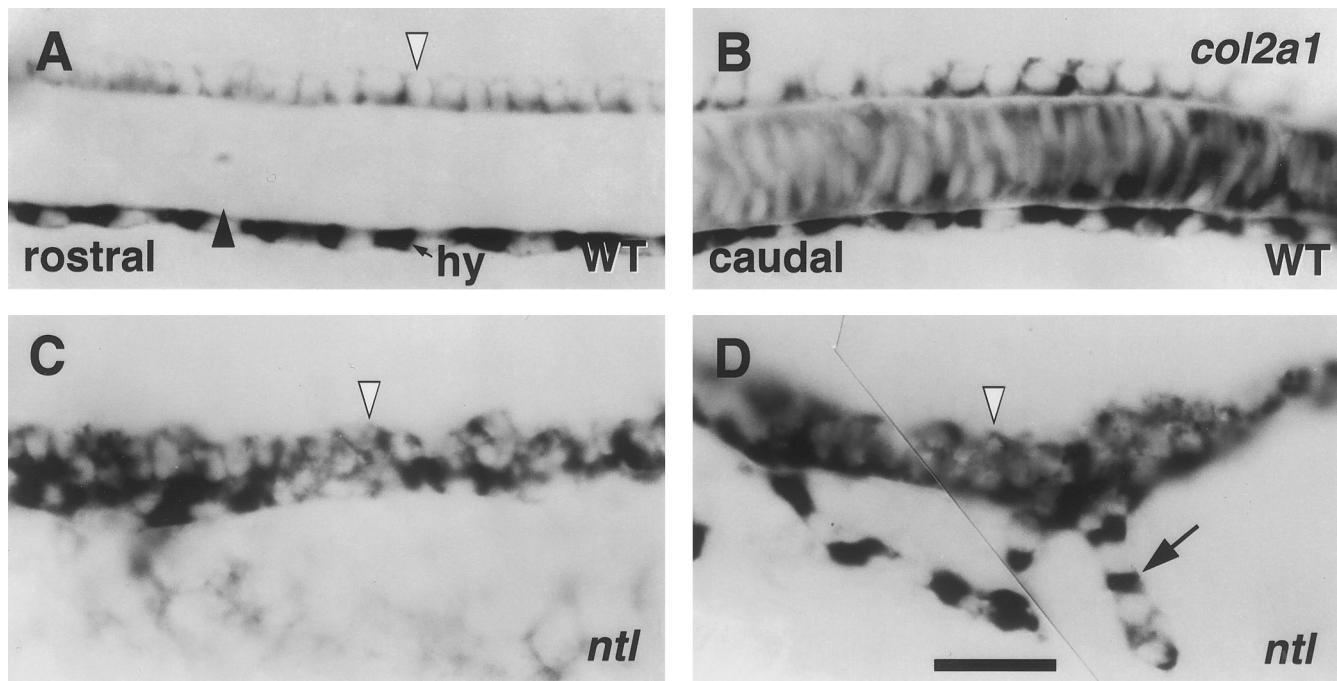
FIG. 7. The floor plate is abnormally broad and cell-rich in *ntl* mutants. Comparisons of expression of *col2a1* in wild types (upper panels) and *ntl* mutants (lower) at rostral (left) and caudal (right) axial levels. Left side views of whole-mounted 24-hr embryos, with anterior to the left and dorsal to the top. RNA *in situ* hybridization with a *col2a1* probe (Yan *et al.,* 1995). Within the spinal cord the wild-type floor plate is a 1-cell-wide row (A, B, white arrowhead). Notochord (dark arrowhead) and hypochord (hy) also express the marker. Often the floor plate in the *ntl* mutant trunk appears irregular (C, D), in a row several cells wide. In addition, ventral projections of cells with the *col2a1* expression characteristic of hypochord (arrow) are often seen in the *ntl* mutant caudal trunk (D). However, expression of *radar,* a marker characteristic of the hypochord in wild-type embryos, was not detected in *ntl* mutants by Rissi *et al.* (1995). Scale bar, 25 μm.

we confirmed by using PCR to genotype the embryos, as described under Materials and Methods).

In summary, the expression studies show that, for most of the trunk midline, *ntl* mutations can strikingly suppress both the muscle and floor plate phenotypes due to loss of *flh* function. Less frequently, in some embryos we observe a local *flh⁻*-like phenotype. Even considering these embryos, however, *ntl* epistasis to *flh* predominates. Nowhere along the midline did we observe a phenotype resembling wild types.

Suppression of cyc by ntl

We recognize *cyc;ntl* double mutants because they exhibit the cyclopic head phenotype that characterizes *cyc⁻*, as well as the tailless phenotype of *ntl⁻* (Fig. 1). Additionally, the notochord is entirely deleted (Fig. 8), just as in *ntl* mutants.

The floor plate phenotypes of *cyc* and *ntl* single mutants contrast more completely than the *flh* and *ntl* comparison just discussed. The trunk floor plate is wider than normal in *ntl⁻* and is missing in *cyc⁻* (Hatta *et al.,* 1991; Odenthal

et al., 1996). We identified floor plate in *cyc;ntl* double mutants (Figs. 8 and 9). This result was not predicted in a straightforward way from our previous interpretations of the single mutant phenotypes (see Discussion) and we examined it thoroughly. The floor plate phenotype is similar or identical in double mutants constructed with any of the three *cyc* alleles in combination with either of the two *ntl* alleles we studied (see Materials and Methods). The floor plate in *cyc;ntl* double mutants is recognizeable by morphology (Nomarski inspection in live embryos) and expresses markers of the wild-type floor plate including *shh* and *col2a1* (Figs. 8 and 9; Krauss *et al.,* 1993; Yan *et al.,* 1995). We observed the same results with additional markers including *axial,* DMgrasp, and keratan sulfate (Strahle *et al.,* 1993; Fashena, 1996; Smith and Watt, 1985).

Axonal pathfinding by axons coursing longitudinally within the ventral central nervous system, normally beside the floor plate, is also defective in *cyc* single mutants (Hatta *et al.,* 1992, Bernhardt *et al.,* 1992a, b). Mosaic analysis has shown that this axonal phenotype is nonautonomous; pathfinding can be locally rescued by cell transplantation to construct genetic mosaics with a stretch of wild-type
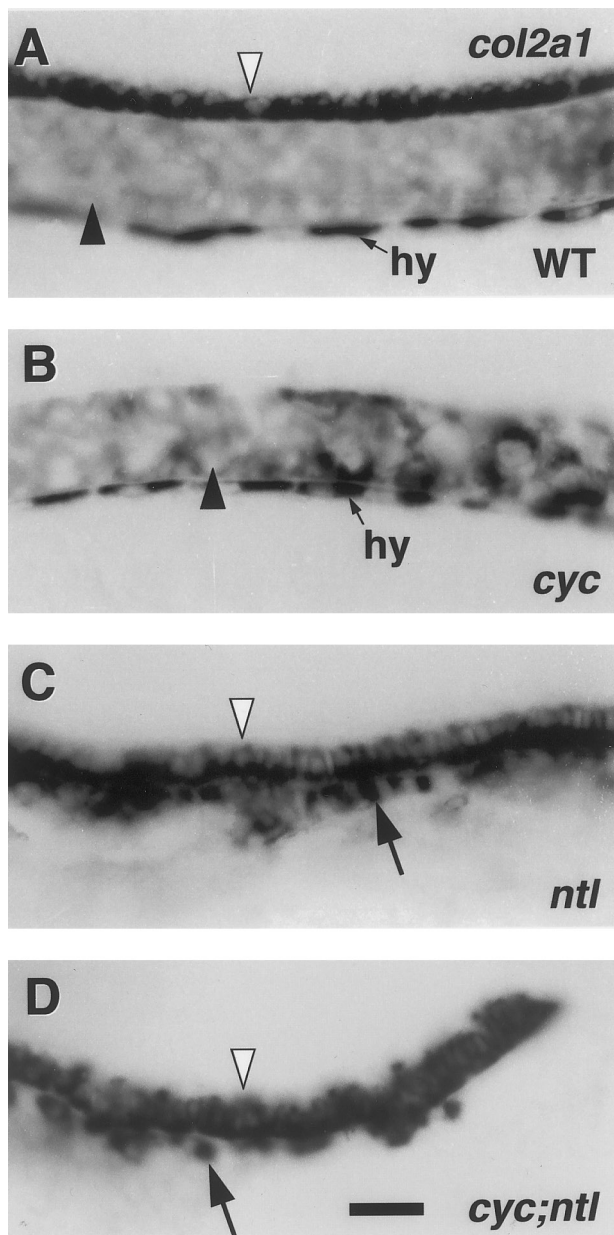
FIG. 9. Midline expression of *shh* in *ntl* mutants (A) and *cyc;ntl* double mutants (B) detected by RNA *in situ* hybridization. Left side views of the trunk of whole-mounted 24-hr embryos, with anterior to the left and dorsal to the top. In *ntl* mutants, *shh* transcripts are present in floor plate (white arrowhead) and in a few cells beneath the spinal cord (arrow). *cyc;ntl* double mutants only show floor plate labeling, present in approximately a 1-cell-wide row. Scale bar, 25 μm.

FIG. 8. Floor plate but not notochord is present in *cyc;ntl* double mutants. Left side views, with anterior to the left and dorsal to the top of whole-mounted 24-hr embryos. RNA *in situ* hybridization with a *col2a1* probe (Yan *et al.,* 1995). In the wild-type (A) expression is in the notochord (dark arrowhead), in the single row of cells that comprise the floor plate (white arrowhead), and in the hypochord (hy). The floor plate is specifically missing in *cyc⁻* (B). The notochord and possibly hypochord (Rissi *et al.,* 1995) are missing in *ntl⁻* (C), whereas the floor plate is present (arrowhead), as are *col2a1*-expressing cells just ventral to the spinal cord and floorplate (arrow). Floor plate is also present in the *cyc;ntl* double mutant hindbrain and trunk spinal cord (D) but labeling does not extend as far caudal as in *ntl* mutants. Cells beneath the floor plate also label in double mutants but these are fewer in number than in *ntl* single mutants (arrow, compare with C). Scale bar, 25 μm.
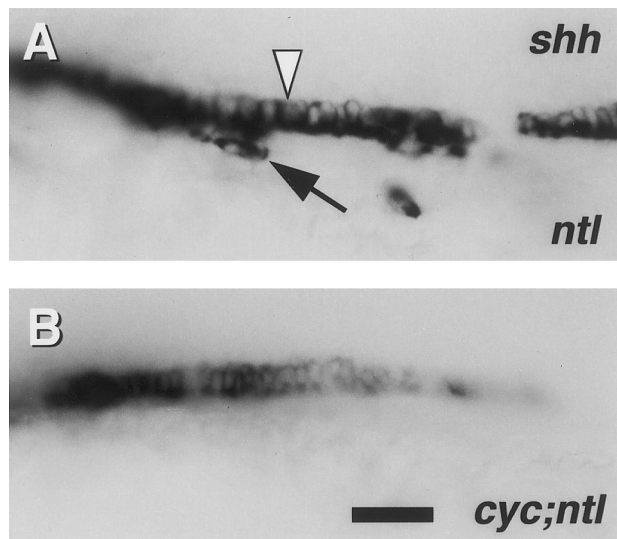
floor plate in an otherwise *cyc* mutant nervous system (Hatta, 1992). We examined axonal pathfinding in *cyc;ntl* double mutants to learn if their floor plate possessed the axonal signaling property (Fig. 10). We observed that within the caudal hindbrain and spinal cord the pathways were normal-looking in *cyc;ntl* double mutants, as in wild-type embryos (not shown) and in *ntl* single mutants.

Together the findings suggest that the floor plate present in the rostral trunk of *cyc;ntl* double mutants is intact morphologically, molecularly, and functionally. However, floor plate is missing at both rostral and caudal extremes of the axis. In wild-type and *ntl⁻* embryos, the floor plate extends rostrally through all of the ventral hindbrain and midbrain. In *cyc;ntl* double mutants, marker expression reveals the floor plate ends rostrally within the hindbrain (see legend to Fig. 10), and, in accord with this, the axonal pathways are disturbed within the hindbrain (in contrast to the spinal cord; Fig. 10). In *ntl⁻* embryos the floor plate is missing in the caudalmost 1–3 body segments, and, just as we showed above for *flh;ntl* double mutants, floor plate markers are not expressed in about the last 8 segments in *cyc;ntl* double mutants.

Our data show that *ntl⁻* acts to suppress the *cyc⁻* absence of floor plate phenotype along a substantial length of the neuraxis, but not the entire length, matching the result obtained with *flh;ntl* double mutants. Hence *ntl* appears epistatic to *cyc* at midbody levels. Even at rostral trunk levels
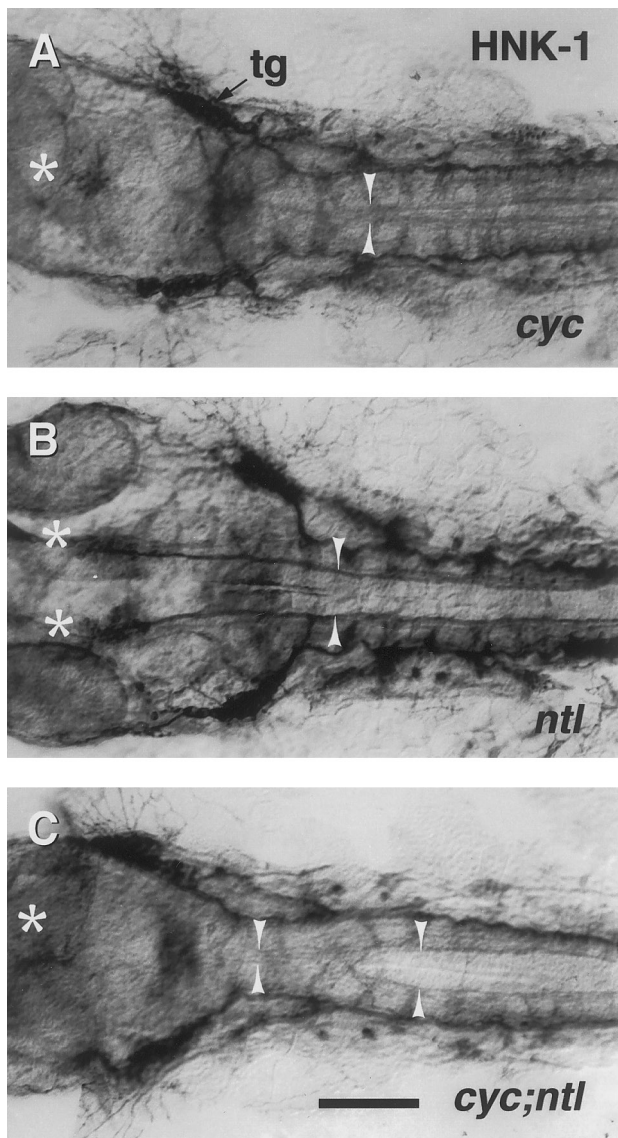
FIG. 10. Floor plate-dependent axonal pathfinding is intact in the caudal hindbrain of *cyc;ntl* double mutants. Dorsal views, with anterior to the left, of the caudal head region of 30-hr embryos, labeled with the zn-12 monoclonal antibody (Trevarrow *et al.,* 1990). This antibody binds the HNK-1 epitope broadly expressed on developing neurons (Metcalfe *et al.,* 1990), including the medial longitudinal fascicles (MLF, arrowheads) which emanate from bilateral neuronal clusters in the midbrain, the nuclei of the MLF (nMLF, asterisks). The MLFs collect additional axons from hindbrain neurons (Metcalfe *et al.,* 1986; Hatta, 1992). The trigeminal ganglion (tg) is approximately at the level of the midbrain–hindbrain boundary. In *cyc* mutants (A) the normally paired nMLF clusters form a single unpaired midline cluster and the MLF axons are poorly defasciculated, present in or near the midline, and often cross the midline (Hatta, 1992). In contrast, in *ntl* mutants (B) the nMLF positions and the MLF axonal trajectories are as in wild-type embryos described previously (Hatta, 1992), and the MLF axons are

where suppression of the *cyc*⁻ phenotype is most complete, the *cyc;ntl* double mutant and *ntl* single mutant phenotypes differ significantly in at least two respects: First, the double mutant floor plate is not several (3–4) cells wide as in *ntl*⁻ but, as revealed by sectioning, and counting *shh*-expressing cells, the *cyc;ntl* double mutant floor plate, is a one cell-wide row, as in wild types (Fig. 11; see legend for quantification). Second, in *ntl*⁻, some cells expressing midline markers are present ventral to the spinal cord, i.e., in the position of the missing notochord (Figs. 7–9; also see Krauss *et al.,* 1993; Shulte-Merker *et al.,* 1994). These cells are decreased in number or are entirely missing in *cyc;ntl* double mutants examined at any stage during the segmentation period or early pharyngula period of development (Figs. 8, 9, and 11).

DISCUSSION

We have characterized double mutants using loss-of-function alleles of *cyc, flh,* and *ntl.* With specific reference to the midline phenotypes at midbody levels, the principal results show that the disturbances due to loss of functions of *cyc* and *flh* are additive, that *ntl* is usually epistatic to *flh,* and that *ntl* is also epistatic to *cyc.* As we discuss below, we interpret these results to mean that *cyc*⁺ and *flh*⁺ do not strongly interact in midline development, that *flh*⁺ and *ntl*⁺ reciprocally influence one another with the *ntl*⁺ influence predominating, and that *cyc*⁺ acts antagonistically to *ntl*⁺. We summarize this model in Fig. 12, which perhaps oversimplifies our view of the genetic interactions involved in midline development, for the circuit will certainly turn out to be a complex network, not a simple pathway, as more genes are analyzed. Our findings also suggest a new role for the *ntl* gene in midline development, namely that it is influencing a cell fate choice between notochord and floor plate, in the same fashion as we have proposed earlier for *flh* to be acting in the choice between notochord and muscle (Halpern *et al.,* 1995; Melby *et al.,* 1996). This role for *ntl* is supported by mouse embryo chimera studies, in which *Brachyury* mutant cells transplanted into wild types were found to preferentially incorporate into the ventral neural tube, including the floor plate, or to incorporate into axial tissue that often fuses with the ventral neural tube (Wilson *et al.,* 1995).

Loss of Midline Tissues and Signaling in cyc;flh Double Mutants

We obtained no evidence for any interactions between *cyc* and *flh* with respect to midline development specifically, at

---

likewise well-fasciculated. In the midbrain and rostral hindbrain, *cyc;ntl* double mutants (C) exhibit defects similar to *cyc* mutants. Correct axonal pathfinding and axonal fasiculation, however, recovers in the hindbrain, the level approximately corresponding to the most rostral region where floor plate is present in these mutants. Scale bar, 100 μm.
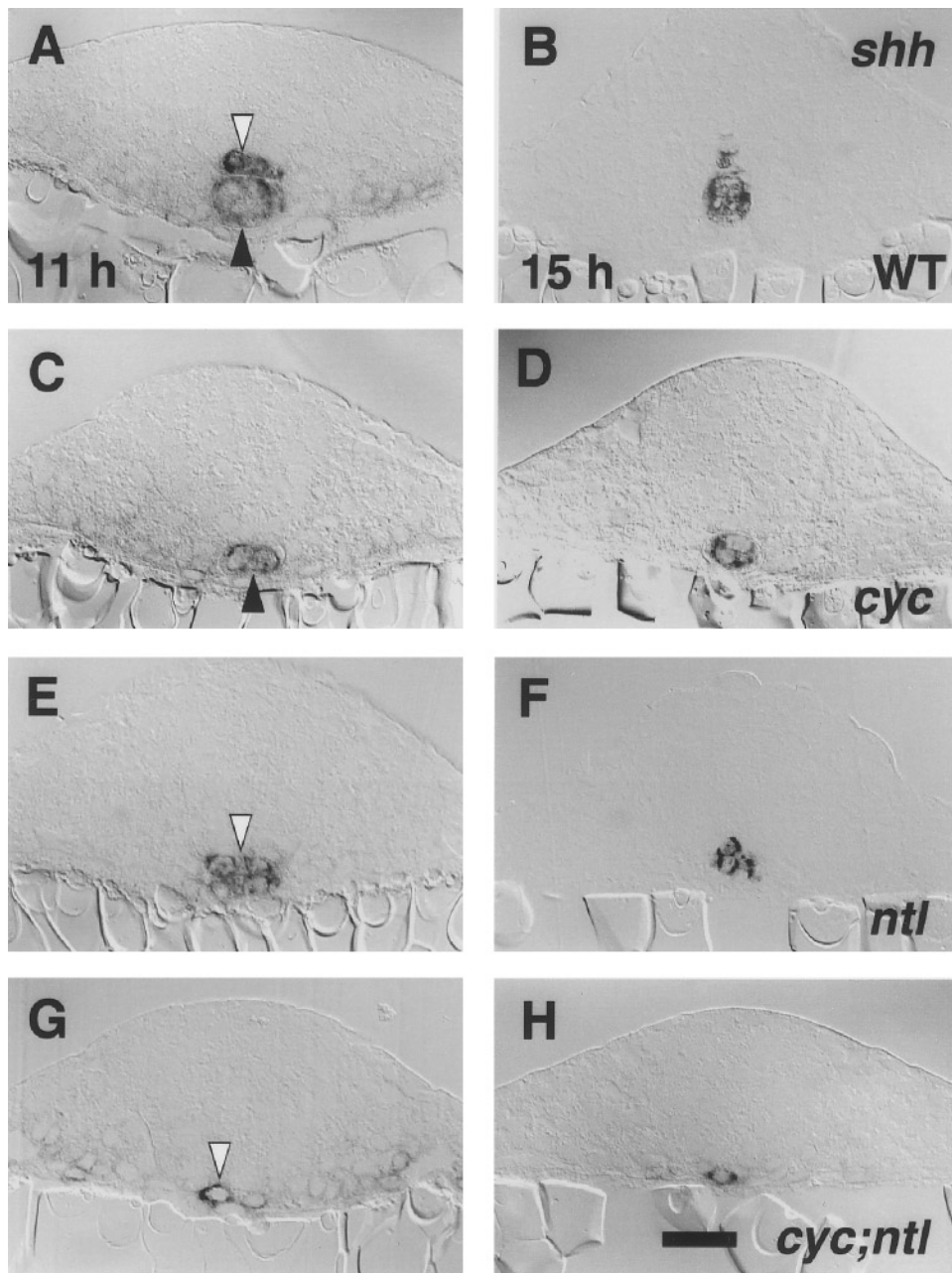
FIG. 11. Cells expressing *shh* are present in a 1-cell-wide row in the trunk midline of *cyc;ntl* double mutants. Transverse sections with dorsal to the top, through 11-hr embryos (4- to 6-somite stage, right panels) and 15-hr embryos (11- to 12-somite stage, left panels). Whole-mount RNA *in situ* hybridization (Krauss *et al.,* 1993) and epon sections of 7 μm were prepared as described under Materials and Methods. *shh* is expressed the floor plate region (white arrowheads) and in the notochord primordium (dark arrowheads) at these stages in wild-type embryos (A, B). Only the notochord is labeled in *cyc* mutants (C, D). In *ntl* mutants (E, F), it was often difficult to assign the position of labeled cells as being within or just beneath the developing spinal cord. Generally only a single labeled cell is observed at the same location in *cyc;ntl* double mutants (G, H). We quantified the difference between *ntl* and *cyc;ntl* mutants by counting *shh*-expressing cells in the midline of sections through the trunk at 11 hr. The number of *shh*-expressing cells per section was determined to be 3.6 $\pm$ 0.4 (mean $\pm$ SEM) for *ntl* mutants (n = 3 embryos, 86 sections total) and 1.2 $\pm$ 0.1 for *cyc;ntl* mutants (n = 3 embryos, 65 sections). The difference is significant ($P < 0.05$; from a t test assuming unequal variances). Scale bar, 25 μm.

$$cyc$$
$$\perp$$
floor
plate $\vdash$ ntl
genes
$$\updownarrow$$
$$flh \dashv \begin{array}{l}\text{muscle}\\ \text{genes}\end{array}$$
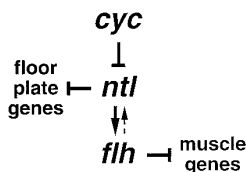
FIG. 12. Model for genetic interactions in the trunk midline. The wild-type alleles of the genes are shown, with both *ntl* and *flh* functioning within the gastrula domain of cells that normally develop as notochord. *cyc* antagonizes *ntl* function (not expression; see text) in the floor plate domain. *ntl* antagonizes floor-plate-specific regulatory genes, and *flh* antagonizes muscle-specific regulatory genes. *ntl* and *flh* reciprocally interact in a positive fashion, with *ntl* occupying a largely upstream position. The model does not explain the curious observation that suppression by *ntl⁻* of the floor-plate-deficient phenotypes of both *cyc⁻* and *flh⁻* does not extend to the more caudal trunk levels.

any body level. Rather the double mutant midline phenotype appears strictly additive: The *cyc;flh* double mutants develop neither notochord nor floor plate at any axial level. Among all the single mutants and double mutant combinations we have studied, midline development is most severely deficient when both *cyc* and *flh* lack function.

The embryonic midline is an important signaling center, in vertebrates and *Drosophila* alike (Jessell and Dodd, 1992; Placzek, 1995; Cossu *et al.,* 1996; Golembo *et al.,* 1996). Hence one expects that the *cyc;flh* double mutant would have phenotypes reflecting the disruption in signaling. In accordance, we observed a number of patterning disturbances in nonmidline cell types in the hindbrain and spinal cord of the *cyc;flh* double mutants. Previous mosaic analyses suggest that the changes in the central nervous system in *cyc* single mutants are nonautonomous (Hatta, 1992). The ventral CNS changes occur outside of the domain of expression (and thus of direct function) of *flh* as well. Hence we think it likely that neural phenotypes not involving the midline in *cyc;flh* double mutants are nonautonomous. These nonmidline phenotypes can be quite severe, revealing synergism in the action of the two genes. The disruption of the patterning of ic interneurons in the caudal hindbrain is a remarkable case in point (Fig. 4). The effect of either single mutant is mild, but in combination the patterning is markedly deficient. As discussed fully in the accompanying paper, it would seem that the synergism we observe reflects parallel signaling roles of the floor plate and notochord, possibly mediated by secretion of Hedgehog proteins (Beattie *et al.,* 1997).

Reciprocal Interactions of flh and ntl in the Notochord Domain

We have interpreted the *flh;ntl* double mutant phenotype to mean that *ntl* is usually epistatic to *flh* with respect to

midline development, but that occasionally the epistasis is reversed. The wild-type phenotype would seemingly result from a delicate balance between the functions of the two genes. Previous expression studies in normal and mutant embryos have shown that both *ntl⁺* and *flh⁺* function directly within the gastrula notochord domain to promote the notochord fate (Schulte-Merker *et al.,* 1994; Talbot *et al.,* 1995; Melby *et al.,* 1997). Furthermore, studies in *ntl* and *flh* single mutants show that the genes reciprocally depend on one another in order to maintain expression in the developing notochord (Talbot *et al.,* 1995; Melby *et al.,* 1997). Hence, a balance in the interactions of these two genes, as revealed in our *flh;ntl* double mutant studies, is not unexpected. Putting the results together suggests that *ntl* and *flh* interact in a positive regulatory feedback loop that is active in the notochord domain specifically, and in which *ntl* predominates (Fig. 12, and see below).

cyc May Act Antagonistically upon ntl

cyc;ntl double mutants possess a floor plate at stages and body levels where floor plate is missing in *cyc* single mutants. The double mutant floor plate appears normal in expression of marker genes and in signaling axonal pathfinding, presumably mediating this effect through local release of chemoattractive and chemorepulsive molecules (reviewed by Colamarino and Tessier-Lavigne, 1995; Keynes and Cook, 1995). Whereas *cyc⁺* is necessary for floor plate development in the wild-type genetic background (and at the stages and body levels we consider), our findings establish that *cyc⁺* is not required if *ntl* also does not function. *ntl⁺*, in turn, is required for a differentiated notochord to develop, but not for the floor plate, since the floor plate is present, indeed is expanded, in *ntl* single mutants. Hence, we can interpret the epistasis to mean that *ntl⁺* acts to antagonize genes specifying floor plate development, and that *cyc⁺* is functioning antagonistically to *ntl,* as in Fig. 12.

One way that *cyc⁺* could antagonize *ntl* function is by directly repressing *ntl* expression. However, Ntl protein expression is slightly reduced in *cyc⁻* notochord precursor cells during late gastrulation and segmentation (Warga, 1996). No expanded *ntl* RNA expression is detected during early segmentation in *cyc⁻* by *in situ* hybridization (S.L.A., unpublished observations). These findings suggest that *ntl* function, rather than expression, is being repressed by *cyc⁺,* or that *cyc⁺* is acting on a downstream target of *ntl.*

ntl May Function in Midline Cell Fate Choice

We proposed earlier that in the absence of function of *ntl* (the homolog of *Brachyury*) undifferentiated notochord precursor cells are present beneath the neural tube that can induce floor plate development (Halpern *et al.,* 1993). Conlon *et al.* (1995) have also argued from expression studies that notochord precursor cells form correctly in mouse *Brachyury* mutants, but then fail to differentiate further.

However, such proposals do not explain why excessive amounts of floor plate are present in *ntl* mutants (Odenthal *et al.,* 1996; this study) nor why *any* floor plate is present in *cyc;ntl* double mutants, particularly in the near-absence of postulated signaling notochord precursor cells beneath the floor plate (e.g., Fig. 9). The *flh;ntl* double mutant phenotype is also not predicted: Assuming notochord precursor cells to be correctly specified in *ntl* mutants, then in *flh;ntl* double mutants we expected they would be respecified toward muscle (Halpern *et al.,* 1995, Melby *et al.,* 1996), and hence the phenotype would resemble *flh⁻*. However, we observed a midline phenotype more closely resembling *ntl⁻*. In particular, excess floor plate is present along most of the length of trunk in *flh;ntl* double mutants. Additionally, new findings cast further doubt on the postulate that the cells in the midline in *ntl* mutants are correctly specified toward notochord development: they express *tiggy winkle hedgehog* (T. Wu, S. Ekker, and M.E.H., unpublished observations), a gene expressed in the developing floor plate in the wild-type embryo (Ekker *et al.,* 1995).

Suppose, alternatively, that in the early organizer region of wild-type embryos *ntl⁺* functions as a switch in a cell fate choice between the notochord and floor plate. The excess floor plate in *ntl* mutants would then be due to cells in the early notochord domain being misrouted toward floor plate development. The cells earlier proposed to be notochord precursors might instead be ectopic floor plate cells, a subset of cells deriving from the notochord fate map domain (the others being present within the expanded *ntl⁻* floor plate). These postulates are consistent with lineage tracing in *ntl* mutants (Halpern *et al.,* 1993; Melby *et al.,* 1996), and with previous expression studies, e.g., of *axial* (HNF3b, Strahle *et al.,* 1993) and *shh* (Krauss *et al.,* 1993), markers which are expressed by *both* developing floor plate and notochord in wild-type embryos. The markers studied by Conlon *et al.* (1995) in mouse *Brachyury* mutants also do not distinguish between notochord and floor plate precursors; indeed, morphological examinations and chimera studies conducted in the mouse suggest that the same change in cell fate that we have proposed occurs in zebrafish *ntl* mutants may also occur in *Brachyury* mutants (Chesley, 1935; Gruenberg, 1958; Wilson *et al.,* 1995). In addition, during late gastrulation zebrafish *ntl* mutant midline cells fail to express *connexin-43.4,* a gene normally expressed in involuted notochord primordial cells, but not presumptive floor plate cells in the epiblast, at this stage (Essner *et al.,* 1996).

This cell fate choice hypothesis can account for the presence of floor plate in *cyc;ntl* double mutants: One needs to assume that having an ectopic source of floor plate cells can override or bypass the disturbance in floor plate development when *cyc* does not function. Earlier work has shown that *cyc⁺* is not always required for floor plate development (Hatta *et al.,* 1991; Hatta, 1992), which is consistent with our proposal. Furthermore, we note that rostral limit of the floor plate in *cyc;ntl* double mutants is not at the forebrain–midbrain boundary, but in the hindbrain, approximately coinciding with where the notochord ends in wild-type embryos. This difference can easily be accommodated by the cell fate choice hypothesis. Since the notochord domain would be the source of the floor plate cells in the *cyc;ntl* double mutant, rescue would not be expected at levels rostral to where the notochord normally ends.

Finally, to explain the *flh;ntl* double mutant midline phenotype, we consider the postulate that in wild-type embryos *ntl⁺* functions to antagonize floor plate development, just as *flh⁺* functions to antagonize muscle development (Halpern *et al.,* 1995, Melby *et al.,* 1996), and the two activities occur in the same cells at about the same stage. Incorporating the notion that *ntl* functions largely upstream to *flh* (Fig. 12), then in the absence of both functions in the *flh;ntl* double mutant, it is reasonable that most of the notochord domain cells are misrouted toward floor plate rather than muscle.

For *ntl* to act as we propose, in wild-type embryos the gene must be expressed by notochord precursor cells, as is well known (see Herrmann and Kispert, 1994, for review), and be not expressed by cells developing as floor plate. Indeed, *ntl* expression seems to be absent in the developing floor plate, at least at late gastrula stages when the two lineages are distinctive (T. Wu and N. Glickman, unpublished observations). An interesting parallel to our results is a study in *Xenopus* (Rao, 1994) which demonstrates that overexpression of mutant forms of the *Xenopus ntl* homolog, *Xbra,* prevents mesoderm formation and leads instead to neuralization in animal cap assays, in contrast to the mesoderm induction that typically results from overexpression of wild-type *Xbra.* Further tests of the cell fate choice hypothesis, for example involving new cell lineage analyses of the notochord domain in *ntl* mutants, and transplanting cells between *ntl* and wild-type embryos, are ongoing.

ACKNOWLEDGMENTS

REFERENCES

Allende, M. L., and Weinberg, E. S. (1994). The expression pattern of two zebrafish achaete-scute homolog (ash) genes is altered in the embryonic brain of the *cyclops* mutant. *Dev. Biol.* **166,** 509–530.

Avery, L., and Wasserman, S. (1993). Ordering gene function: The interpretation of epistasis in regulatory hierarchies. *Trends Genet.* **8,** 312–316.

Barth, K. A., and Wilson, S. W. (1995). Expression of zebrafish *nk*2.2 is influenced by *sonic hedgehog/vertebrate hedgehog-1* and demarcates a zone of neuronal differentiation in the embryonic forebrain. *Development* **121,** 1755–1768.

Beattie, C. E., Hatta, K., Halpern, M. E., Liu, H., Eisen, J. S., and Kimmel, C. B. (1997). Temporal separation in the specification of primary and secondary motoneurons in zebrafish. *Dev. Biol.* **187,** 171–182.

Bernhardt, R. R., Nguyen, N., and Kuwada, J. Y. (1992a). Growth cone guidance by floor plate cells in the spinal cord of zebrafish embryos. *Neuron* **8,** 869–882.

Bernhardt, R. R., Patel, C. K., Wilson, S. W., and Kuwada, J. Y. (1992b). Axonal trajectories and distribution of GABAergic spinal neurons in wildtype and mutant zebrafish lacking floor plate cells. *J. Comp. Neurol.* **326,** 263–272.

Chesley, P. (1935). Development of the short-tailed mutant in the house mouse. *J. Exp. Zool.* **70,** 429–459.

Chiang, C., Litingtung, Y., Lee, E., Young, K. E., Corden, J. L., Westphal, H., and Beachy, P. A. (1996). Cyclopia and defective axial patterning in mice lacking *Sonic Hedgehog* gene function. *Nature* **383,** 407–413.

Colamarino, S. A., and Tessier-Lavigne, M. (1995). The role of the floor plate in axon guidance. *Annu. Rev Neurosci.* **18,** 497–529.

Conlon, F. L., Sedgwick, S. G., Weston, K. M., and Smith, J. C. (1996). Inhibition of *Xbra* transcription activation causes defects in mesodermal patterning and reveals autoregulation of *Xbra* in dorsal mesoderm. *Development* **122,** 2427–2435.

Conlon, F. L., Wright, C. V. E., and Robertson, E. J. (1995). Effects the *T^{Wis}* mutation on notochord formation and mesodermal patterning. *Mech. Dev.* **49,** 201–209.

Cossu, G., Tajbakhsh, S., and Buckingham, M. (1996). How is myogenesis initiated in the embryo? *Trends Genet.* **12,** 218–223.

Ekker, S. C., Ungar, A. R., Greenstein, P., von-Kessler, D. P., Porter, J. A., Moon, R. T., and Beachy, P. A. (1995). Patterning activities of the vertebrate hedgehog proteins in the developing eye and brain. *Curr. Biol.* **5,** 944–955.

Essner, J. J., Laing, J. G., Beyer, E. C., Johnson, R. G., and Hackett, P. B. (1996). Expression of zebrafish *connexin 43.4* in the notochord and tail bud of wild-type and mutant *no tail* embryos. *Dev. Biol.* **177,** 449–462.

Fashena, D. S. (1996). ''A Neuron's Reach Can Exceed its GRASP: Expression of a Cell Adhesion Molecule in the Zebrafish Embryo.'' Ph.D. thesis, University of Oregon.

Golembo, M., Raz, E., and Shilo, B. Z. (1996). The *Drosophila* embryonic midline is the site of spitz processing and induces activation of the EGF receptor in the ventral ectoderm. *Development* **122,** 2263–3370.

Gont, L. K., Fainsod, A., Kim, S. H., and DeRobertis, E. M. (1996). Overexpression of the homeobox gene *Xnot-2* leads to notochord formation in *Xenopus. Dev. Biol.* **174,** 174–178.

Gont, L. K., Steinbeisser, H., Blumberg, B., and DeRobertis, E. M. (1993). Tail formation as a continuation of gastrulation: The mul-

tiple cell populations of the *Xenopus* tailbud derive from the late blastopore lip. *Development* **119,** 991–1004.

Gruenberg, H. (1958). Genetical studies on the skeleton of the mouse. XXIII. The development of *Brachyury* and *Anury. J. Embryol. Exp. Morphol.* **6,** 424–443.

Halpern, M. E., Ho, R. K., Walker, C., and Kimmel, C. B. (1993). Induction of muscle pioneers and floor plate is distinguished by the zebrafish *no tail* mutation. *Cell* **75,** 99–111.

Halpern, M. E., Thisse, C., Ho, R. K., Thisse, B., Riggleman, B., Trevarrow, B., Weinberg, E. S., Postlethwait, J. H., and Kimmel, C. (1995). Cell-autonomous shift from axial to paraxial mesodermal development in zebrafish *floating head* mutants. *Development* **121,** 4257–4264.

Hammerschmidt, M., Brook, A., and McMahon, A. P. (1997). The world according to *hedgehog. Trends Genet.* **13,** 14–21.

Harada, Y., Yasuo, H., and Satoh, N. (1995). A sea urchin homologue of the chordate *Brachyury* (*T*) gene is expressed in the secondary mesenchyme founder cells. *Development* **121,** 2747–2754.

Hatta, K. (1992). Role of the floor plate in axonal patterning in the zebrafish CNS. *Neuron* **9,** 629–642.

Hatta, K., Kimmel, C. B., Ho, R. K., and Walker, C. (1991). The *cyclops* mutation blocks specification of the floor plate of the zebrafish central nervous system. *Nature* **350,** 339–341.

Hatta, K., Püschel, A. W., and Kimmel, C. B. (1994). Midline signaling in the primordium of the zebrafish anterior central nervous system. *Proc. Natl. Acad. Sci. USA* **91,** 2061–2065.

Hauptmann, G., and Gerster, T. (1996). Complex expression of the *zp-50* pou gene in the embryonic zebrafish brain is altered by overexpression of *sonic hedgehog. Development* **122,** 1769–1780.

Herrmann, B. G. (1991). Expression pattern of the *Brachyury* gene in whole-mount *T^{wis}/T^{wis}* mutant embryos. *Development* **113,** 913–917.

Herrmann, B. G., and Kispert, A. (1994). The *T* genes in embryogenesis. *Trends Genet.* **10,** 280–286.

Holland, P. W. H., Koschorz, B., Holland, L. Z., and Herrmann, B. G., (1995). Conservation of *Brachyury* (*T*) genes in amphioxus and vertebrates: Developmental and evolutionary implications. *Development* **121,** 4283–4291.

Jessell, T. M., and Dodd, J. (1992). Midline signals that control the dorso-ventral polarity of the neural tube. *Semin. Neurosci.* **4,** 317–325.

Johnson, S. L., Gates, M. A., Johnson, M., Talbot, W. S., Horne, S., Baik, K., Rude, S., Wong, J. R., and Postlethwait, J. H. (1996). Centromere-linkage analysis and consolidation of the zebrafish genetic map. *Genetics* **142,** 1277–1288.

Johnson, S. L., Midson, C. N., Ballinger, E. W., and Postlethwait, J. H. (1994). Identification of RAPD primers that reveal extensive polymorphisms between laboratory strains of zebrafish. *Genomics* **19,** 152–156.

Kanki, J. P., Chang, S., and Kuwada, J. Y. (1994). The molecular cloning and characterization of potential DM-GRASP homologs in zebrafish and mouse. *J. Neurobiol.* **25,** 831–835.

Keynes, R., and Cook, G. M. W. (1995). Axon guidance molecules. *Cell* **83,** 161–169.

Kimmel, C. B., Ballard, W. W., Kimmel, S. R., Ullmann, B., and Schilling, T. (1995). Stages of embryonic development of the zebrafish. *Dev. Dyn.* **203,** 253–310.

Kispert, A., and Herrmann, B. G. (1993). The *Brachyury* gene encodes a novel DNA binding protein. *EMBO J.* **12,** 3211–3220.

Kispert, A., and Herrmann, B. G. (1994). Immunohistochemical

analysis of the *Brachyury* protein in wild-type and mutant mouse embryos. *Dev. Biol.* **161,** 179–193.

Kispert, A., Herrmann, B. G., Leptin, M., and Reuter, R. (1994). Homologs of the mouse Brachyury gene are involved in the specification of posterior terminal structures in *Drosophila, Tribolium,* and *Locusta. Genes Dev.* **8,** 2137–2150.

Kispert, A., Koschorz, B., and Herrmann, B. G. (1995a). The T protein encoded by *Brachyury* is a tissue-specific transcription factor. *EMBO J.* **14,** 4763–4772.

Kispert, A., Ortner, H., Cooke, J., and Herrmann, B. G. (1995b). The chick *Brachyury* gene: Developmental expression pattern and response to axial induction by localized activin. *Dev. Biol.* **168,** 406–415.

Knapik, E. W., Goodman, A., Atkinson, O. S., Roberts, C. T., Shiozawa, M., Sim, C. U., Weksler-Zangen, S., Trolliet, M. R., Futrell, C., Innes, B. A., Koike, G., McLaughlin, M. G., Pierre, L., Simon, J. S., Vilallonga, E., Roy, M., Chiang, P.-W., Fishman, M. C., Driever, W., and Jacob, H. J. (1996). A reference cross DNA panel for zebrafish (*Danio rerio*) anchored with simple sequence length polymorphisms. *Development* **123,** 451–460.

Knezevic, V., Ranson, M., and Mackem, S. (1995). The organizer-associated chick homeobox gene, *Gnot1,* is expressed before gastrulation and regulated synergistically by activin and retinoic acid. *Dev. Biol.* **171,** 458–470.

Krauss, S., Concordet, J.-P., and Ingham, P. W. (1993). A functionally conserved homolog of the *Drosophila* segment polarity gene *hh* is expressed in tissues with polarizing activity in zebrafish embryos. *Cell* **75,** 1431–1444.

Lemaire, P., and Kodjabachian, L. (1996). The vertebrate organizer: Structure and molecules. *Trends Genet.* **12,** 525–531.

Macdonald, R., Barth, K. A., Xu, Q., Holder, N., Mikkola, I., and Wilson, S. W. (1995). Midline signalling is required for Pax gene regulation and patterning of the eyes. *Development* **121,** 3267–3278.

Melby, A. E., Kimelman, D., and Kimmel, C. B. (1997). Spatial regulation of floating head expression in the developing notochord. *Dev. Dyn.* In press.

Melby, A. E., Warga, R. M., and Kimmel, C. B. (1996). Specification of cell fates at the dorsal margin of the zebrafish gastrula. *Development* **122,** 2225–2237.

Mendelson, B. (1986). Development of reticulospinal neurons of the zebrafish. II. Early axonal outgrowth and cell body position. *J. Comp. Neurol.* **251,** 172–184.

Metcalfe, W. K., Mendelson, B., and Kimmel, C. B. (1986). Segmental homologies among reticulospinal neurons in the hindbrain of the zebrafish larva. *J. Comp. Neurol.* **251,** 147–159.

Metcalfe, W. K., Myers, P. Z., Trevarrow, B., Bass, M. B., and Kimmel, C. B. (1990). Primary neurons that express the L2/HNK-1 carbohydrate during early development in the zebrafish. *Development* **110,** 491–504.

Odenthal, J., Haffter, P., Vogelsang, E., Brand, M., van Eeden, F. J. M., Furutani-Seiki, M., Granato, M., Hammerschmidt, M., Heisenberg, C.-P., Jiang, Y.-J., Kane, D. A., Kelsh, R. N., Mullins, M. C., Warga, R. M., Allende, M., L., Weinberg, E. S., and Nüsslein-Volhard, C. (1996). Mutations affecting the formation of the notochord in the zebrafish, *Danio rerio. Development* **123,** 103–115.

Oxtoby, E., and Jowett, T. (1993). Cloning of the zebrafish *krox-20* gene (*krx-20*) and its expression during hindbrain development. *Nucleic Acids Res.* **21,** 1087–1095.

Placzek, M. (1995). The role of the notochord and floor plate in inductive interactions. *Curr. Opin. Genet. Dev.* **5,** 499–506.

Placzek, M., Jessell, T. M., and Dodd, J. (1993). Induction of floor plate by contact-dependent homeogenetic signals. *Development* **117,** 205–218.

Postlethwait, J. H., Johnson, S. L., Midson, C. N., Talbot, W. S., Gates, M., Ballinger, E. W., Africa, D., Andrews, R., Carl, T., Eisen, J. S., Horne, S., Kimmel, C. B., Hutchinson, M., Johnson, M., and Rodriquez, A. (1994). A genetic linkage map for the zebrafish. *Science* **264,** 699–703.

Rao, Y. (1994). Conversion of a mesodermalizing molecule, the *Xenopus Brachyury* gene, into a neuralizing one. *Genes Dev.* **8,** 939–947.

Rashbass, P., Wilson, V., Rosen, B., and Beddington, R. S. P. (1994). Alterations in gene expression during mesoderm formation and axial patterning in *Brachyury* (*T*) embryos. *Int. J. Dev. Biol.* **38,** 35–44.

Rissi, M., Wittbrodt, J., Delot, E., Naegeli, M., and Rosa, F. M. (1995). Zebrafish *radar,* a new member of the *TGF-β* superfamily defines dorsal regions of the neural plate and the embryonic retina. *Mech. Dev.* **49,** 223–234.

Schulte-Merker, S., Ho, R. K., Herrmann, B. G., and Nüsslein-Volhard, C. (1992). The protein product of the zebrafish homologue of the mouse *T* gene is expressed in nuclei of the germ ring and the notochord of the early embryo. *Development* **116,** 1021–1032.

Schulte-Merker, S., van Eeden, F. J. M., Halpern, M. E., Kimmel, C. B., and Nüsslein-Volhard, C. (1994). no tail (*ntl*) is the zebrafish homologue of the mouse *T* (*Brachyury*) gene. *Development* **120,** 1009–1115.

Shih, J., and Fraser, S. E. (1995). Distribution of tissue progenitors within the shield region of the zebrafish gastrula. *Development* **121,** 2755–2765.

Smith, J. C., and Watt, F. M. (1985). Biochemical specificity of *Xenopus* notochord. *Differentiation* **29,** 109–115.

Smith, J. C., Price, B. M., Green, J. B., Weigel, D., and Herrmann, B. G. (1991). Expression of a *Xenopus* homolog of *Brachyury* (*T*) is an immediate-early response to mesoderm induction. *Cell* **67,** 79–87.

Stachel, S. E., Grunwald, D. J., and Myers, P. Z. (1993). Lithium perturbation and *goosecoid* expression identify a dorsal specification pathway in the pregastrula zebrafish. *Development* **117,** 1261–1274.

Stein, S., and Kessel, M. (1995). A homeobox gene involved in node, notochord and neural plate formation of chick embryos. *Mech. Dev.* **49,** 37–48.

Stein, S., Knut, N., and Kessel, M. (1996). Differential activation of the clustered homeobox genes *CNOT2* and *CNOT1* during notogenesis in the chick. *Dev. Biol.* **180,** 519–533.

Strahle, U., Blader, P., Henrique, D., and Ingham, P. W. (1993). *Axial,* a zebrafish gene expressed along the developing body axis, shows altered expression in *cyclops* mutant embryos. *Gene Dev.* **7,** 1436–1446.

Talbot, W. S., Trevarrow, B., Halpern, M. E., Melby, A. E., Farr, G., Postlethwait, J. H., Jowett, T., Kimmel, C. B., and Kimelman, D. (1995). A homeobox gene essential for zebrafish notochord development. *Nature* **378,** 150–157.

Thisse, C., Thisse, B., Halpern, M. E., and Postlethwait, J. H. (1994). *goosecoid* expression in neurectoderm and mesoderm is disrupted in zebrafish *cyclops* gastrulas. *Dev. Biol.* **164,** 420–429.

Thisse, C., Thisse, B., Schilling, T., and Postlethwait, J. H. (1993).

Structure of the zebrafish *snail* gene and its expression in wild-type, *spadetail* and *no tail* mutant embryos. *Development* **119,** 1203–1213.

Toyama, R., Curtiss, P. E., Otani, H., Kimura, M., Dawid, I. B., and Taira, M. (1995). The LIM class homeobox gene *lim5:* Implied role in CNS patterning in *Xenopus* and zebrafish. *Dev. Biol.* **170,** 583–593.

Trevarrow, B., Marks, D. L., and Kimmel, C. B. (1990). Organization of hindbrain segments in the zebrafish embryo. *Neuron* **4,** 669–679.

Ungar, A. R., Kelly, G. M., and Moon, R. T. (1995). *Wnt4* affects morphogenesis when misexpressed in the zebrafish embryo. *Mech. Dev.* **52,** 153–164.

von Dassow, G., Schmidt, J. E., and Kimelman, D. (1993). Induction of the *Xenopus* organizer: Expression and regulation of *Xnot,* a novel FGF and activin-regulated homeobox gene. *Genes Dev.* **7,** 355–366.

Warga, R. M. (1996). ''Origin and Specification of the Endoderm in the Zebrafish.'' Ph.D. dissertation, University of Tübingen, Germany.

Weinberg, E. S., Allende, M. L., Kelly, C. S., Abdelhamid, A., Murakami, T., Andermann, P., Doerre, O. G., Grunwald, D. J., and Riggleman, B. (1996). Developmental regulation of zebrafish *MyoD* in wild-type, *no tail* and *spadetail* embryos. *Development* **122,** 271–280.

Westerfield, M. (1994). ''The Zebrafish Book.'' University of Oregon Press, Eugene.

Wilkinson, D. G., Bhatt, S., and Herrmann, B. G. (1990). Expression pattern of the mouse *T* gene and its role in mesoderm formation. *Nature* **343,** 657–658.

Wilson, V., Manson, L., Skarnes, W. C., and Beddington, R. P. (1995). The *T* gene is necessary for normal meosdermal morphogenetic cell movements during gastrulation. *Development* **121,** 877–886.

Yamada, T., Pfaff, S. L., Edlund, T., and Jessell, T. M. (1993). Control of cell pattern in the neural tube: Motor neuron induction by diffusible factors from notochord and floor plate. *Cell* **73,** 673–686.

Yamada, T., Placzek, M., Tanaka, H., Dodd, J., and Jessell, T. M. (1991). Control of cell pattern in the developing nervous system: Polarizing activity of the floor plate and notochord. *Cell* **64,** 635–647.

Yan, Y.-L., Hatta, K., Riggleman, B., and Postlethwait, J. H. (1995). Expression of a *type II collagen* gene in the zebrafish embryonic axis. *Dev. Dyn.* **203,** 363–376.

Yasuo, H., and Satoh, N. (1993). Function of vertebrate *T* gene. *Nature* **364,** 582–583.

Yasuo, H., and Satoh, N. (1994). An ascidian homolog of the mouse *Brachury* (*T*) gene is expressed exclusively in notochord cells at the fate-restricted stage. *Dev. Growth Differ.* **36,** 9–18.